

Autonomous Intelligent Technology for Three-Steel Temperature Measurement Using Suspended-Rail Infrared Thermometry

Qiang Yu¹, Qing Wei², Yuechao Guan³, Yanan Zhang⁴, Weiming Li⁵,
Lijun Zhao⁶ and Xiangzhou Miao⁷

1, 3, 7. Engineers

2. Senior Engineer

4. President

Zhengzhou Non-ferrous Metals Research Institute of Chalco (ZRI), Zhengzhou, China

5. Plant Director

6. Engineer

Chinalco Baotou, Baotou, China

Corresponding author: qing_wei@chinalco.com.cn

<https://doi.org/10.71659/icsoba2025-al047>

Abstract

To address key challenges in monitoring the “three steel temperatures” – sidewall, collector bar, and potshell bottom plate – of aluminium reduction cells, such as high labour intensity, large data dispersion, prominent safety risks, and low efficiency, this study innovatively developed an overhead rail infrared temperature inspection system. By suspending an inspection rail and device beneath the bottom beam of the cell, and integrating spatial positioning, infrared temperature sensing, wireless communication, and adaptive drive modules, the system establishes a triune automated inspection mechanism of “positioning-acquisition-analysis”. Industrial tests on a 400 kA electrolytic cell show that the system inspects 144 marked points in just 240 s, achieving a 300 % improvement in efficiency compared to manual inspection. It also delivers a positioning accuracy of ± 1 cm and a temperature measurement accuracy of ± 1 °C. Compared to manual measurement, the average standard deviation of the collected data decreased from 6.2 to 0.7, reducing data dispersion by 88.7 %. In conclusion, the overhead rail inspection system significantly improves inspection efficiency and accuracy, enhances safe operation and control of electrolytic cells, and meets the monitoring requirements for the steel temperatures of the cells.

Keywords: Aluminium reduction cell, Three steel temperature measurement, Intelligent inspection.

1. Introduction

As the core equipment in aluminium smelting, aluminium reduction cells have three critical temperature measurement points – the sidewall, collector bar, and potshell bottom – collectively known as the “three steel temperatures” [1]. Real-time and precise monitoring of these three key areas is of great importance for analysing the temperature field distribution within the cell, preventing premature cell failure, and extending the service life of the cell [2, 3].

In traditional methods, the three-steel temperatures are measured manually using handheld infrared thermometers, which requires point-by-point inspection. This approach is labour-intensive and inefficient, and poses safety threats to inspectors, especially in emergency scenarios [4]. To address this issue, some studies have explored installing online temperature measurement devices on the sidewalls of electrolytic cells. However, harsh conditions such as high temperature, strong magnetic fields, and heavy dust make it difficult to install and secure temperature-sensing cables and probes. These components are prone to detachment or damage, resulting in substantial measurement errors [5]. Moreover, given the tens of thousands of temperature measurement

points in potline the installation and maintenance costs of the required distributed optical cable acquisition devices are too high, hindering large-scale application [6, 7].

Ground robot-based temperature measurement solutions face several challenges. On the one hand, the confined space beneath the electrolytic cells limits the manoeuvrability of large robots. On the other hand, the high-temperature slag produced by the cells can corrode both the robots and their sensors, and also block their paths, affecting normal operation [8]. In addition, the strong magnetic field environment interferes with signal transmission, resulting in inaccurate positioning, frequent equipment failures, increased maintenance costs, and reduced operational efficiency [9].

To solve the challenge of accurately measuring the three-steel temperatures of the cells, this paper proposes an innovative integrated solution that combines an overhead rail inspection device with infrared temperature measurement technology. A dedicated monitoring and control system for the three-steel temperatures is designed and developed to enable real-time, dynamic monitoring and precise regulation of critical temperature points within the cell, providing technical support for achieving intelligent and refined management of aluminium electrolysis production processes.

2. Overall System Design

To meet the temperature monitoring requirements under the complex operating conditions of the cells, this paper presents a inhouse-developed overhead rail intelligent inspection robot system, whose overall control architecture is shown in Figure 1. Centred on a modular design, the system consists of two core modules that work in coordination: the inspection robot and the data processing centre. Serving as the sensing terminal, the inspection robot features a lightweight mechanical structure and integrates a drive system and a low-latency communication module, enabling autonomous cruising along preset rail paths and real-time data transmission. A laser ranging module measures the spatial distance between the robot and the target parts of the cell in real time, feeding the data back to the control system. Intelligent algorithms dynamically adjust the focal length of the infrared temperature measurement lens to eliminate measurement errors caused by distance variations.

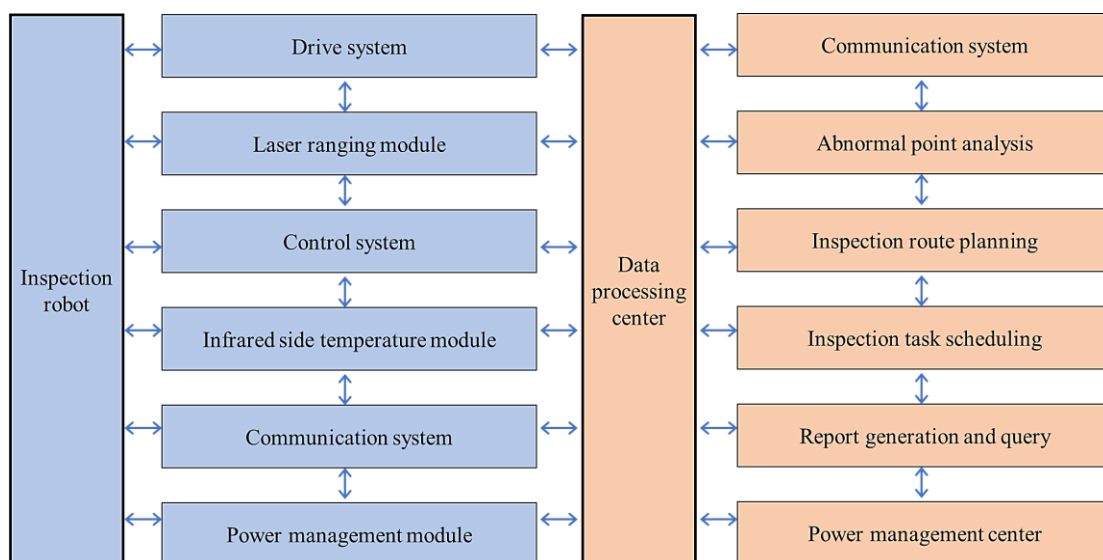


Figure 1. Overall control architecture diagram.

The inspection robot data processing centre serves as the intelligent monitoring hub of the system, integrating core functions such as inspection task planning, data parsing, anomaly detection, and dynamic scheduling. Through industrial-grade data interfaces, the centre receives infrared

temperature data, laser ranging information, and motion status parameters transmitted by the robot in real time, enabling multi-source data parsing and preprocessing. When an abnormal temperature is detected, the centre interrupts the routine inspection workflow and prioritizes redeploying the robot to re-inspect the abnormal point, thereby providing technical support for the safe and stable operation of the cells.

3. System Implementation

3.1 Intelligent Inspection Robot

The intelligent inspection robot adopts a modular architecture that decouples its core functions into three independent systems: drive, control, and communication. These modules operate collaboratively through standardized interfaces. The drive system powers the robot's suspended movement mechanism; the control system generates and executes motion commands; and the communication system enables data exchange and remote transmission between the robot and the computer.

Drive System

The suspended robot is powered by a built-in 24 V lithium battery, allowing continuous operation for more than 3 hours on a full charge. It is equipped with an intelligent power management system that monitors and reports battery status in real time. When the battery level drops below 5 % capacity threshold, the system automatically issues a low-battery warning and initiates an emergency return-to-home procedure.

Control System

Based on preset motion control algorithms, the system generates control commands to drive the actuators, enabling fully autonomous navigation. The system achieves a cruising speed exceeding 0.3 m/s and a positioning accuracy of ± 1 cm, and supports intelligent functions such as scheduled inspection, self-diagnostics, and one-click cruising.

Communication System

The system is equipped with dual independent wireless communication links: the main link (device to host computer) handles the exchange of control commands and status data, while the secondary link (sensor to monitoring terminal) is dedicated to real-time transmission of the "three-steel temperature" data. It offers an effective communication radius of over 300 m and a data transmission rate greater than 100 kbps, with both channels operating in parallel without signal interference.

3.2 Rail Installation Design

The inspection robot rail is made of high-strength metal material and is connected in sections. Using suspension accessories, the rail is suspended beneath the H-beam. Photoelectric position sensors are installed at both the starting and ending points of the rail to enable the robot to identify the starting and ending points of the inspection route.

3.3 Monitoring Module Design

The laser rangefinder emits laser pulse signals via a laser emitter, which are reflected by the target and returned to the receiver. The distance to the target is then calculated based on the speed of light and the signal's travel time, providing a reliable spatial positioning basis for subsequent temperature measurement. The infrared thermometer is a non-contact temperature measurement device that supports online measurement and can wirelessly transmit temperature data to the

computer in real time via RS485 communication, enabling operators to perform data analysis and monitoring.

The system is equipped with a circular laser aimer coaxial with the infrared thermometer's temperature sensor. During measurement, the aimer emits two infrared beams, forming two red spots 3 cm apart on the measured steel plate. The system calculates the measured temperature by using the midpoint of the two red spots and the average temperature of the corresponding coaxial circular area, ensuring the stability and accuracy of the temperature data.

3.4 Communication Module Design

The infrared thermometer carried by the inspection robot adopts Modbus RTU as the main communication protocol to establish a communication connection with the host computer. The system uses a mobile computer running the Windows operating system as the controller, with communication and control of the inspection robot handled through inspection robot management software developed on the QT platform. The controller is connected to a LoRa wireless communication adapter via a USB-to-serial cable. This adapter performs signal conversion and handles Modbus RTU protocol-related tasks, including message frame construction, function code processing, and CRC verification. LoRa spread spectrum significantly enhances communication signal transmission distance and penetration while reducing on-site electromagnetic interference. The communication data structure is shown in Figure 2.

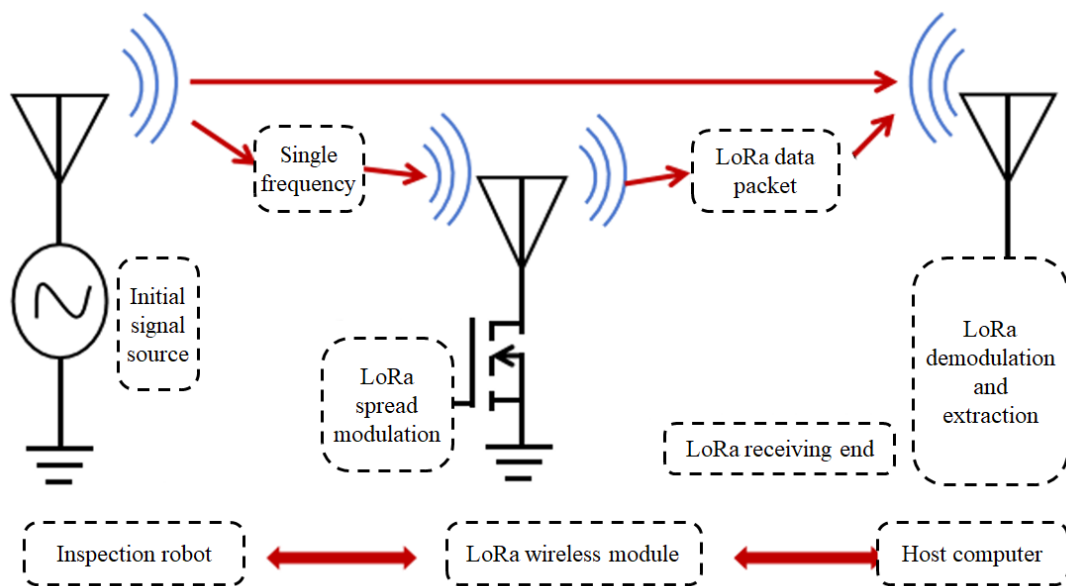


Figure 2. Communication logical diagram of the inspection system.

3.5 Inspection Program Development

Inspection robot testing task management begins with the real-time inspection module, where the system initiates serial communication and completes parameter initialization (including address, baud rate, and data bit settings). The system then enters the inspection setup phase, where users can switch to the parameter setting module for signal configuration, threshold setting, and rate adjustment. After the parameters are set, the system collects temperature and position data while simultaneously activating the inspection path recording function. During the recording process, temperature measurement positions need to be marked. Once path recording is complete, the system saves the inspection route and checks its accuracy: if verified, the inspection task is

initiated; if deviations are detected, it returns to the path recording phase for re-planning, as shown in Figure 3.

During the inspection execution, the system continuously monitors and records data, dynamically displaying the current status through the real-time data interface. Upon task completion, the system automatically compares the current data with historical records and presents the analysis results on a dedicated interface.

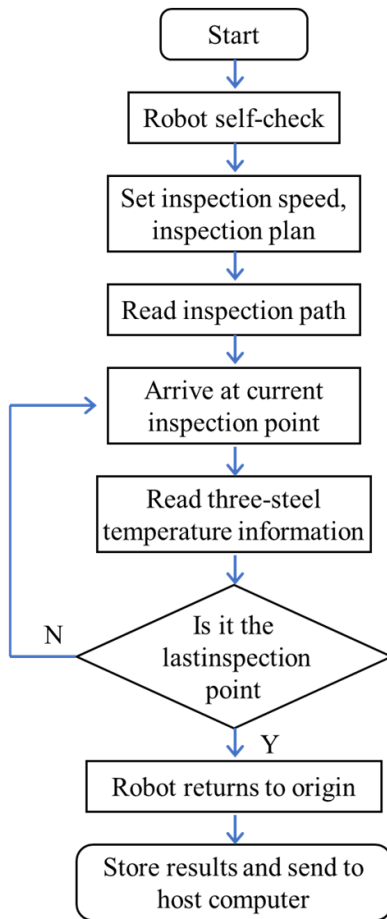


Figure 3. Robot inspection process diagram.

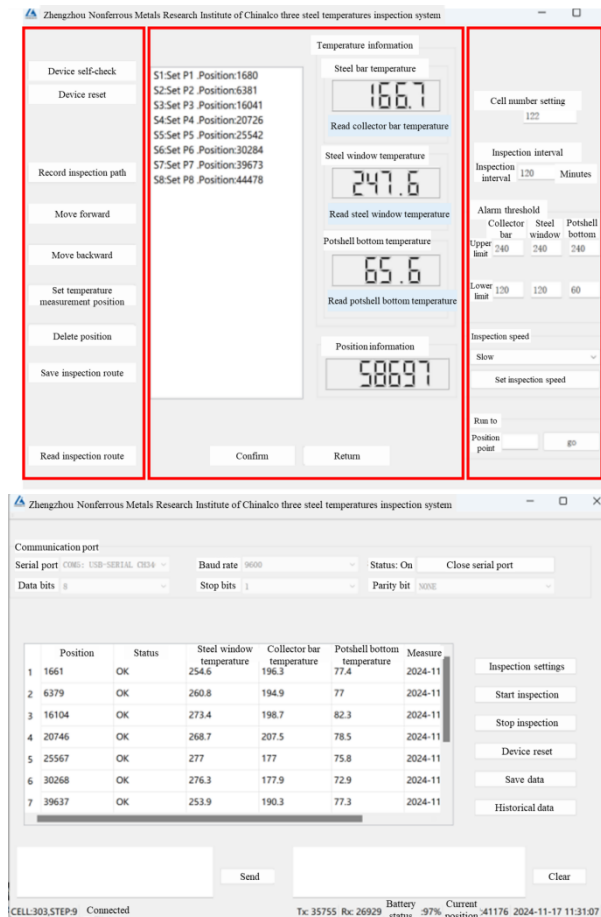


Figure 4. Host computer inspection setup and inspection result interface.

The overhead rail robot is capable of performing specific and customized inspection tasks in specialized environments, equipped with autonomous positioning and navigation capabilities. The parameter setting module, as the core communication component between the controller and the inspection robot, plays a crucial role in rail operation scenarios. It enables personnel to efficiently adjust inspection parameters and operating status, ensuring operational accuracy and task optimization. As shown in Figure 4, this module consists of the inspection setup interface and the real-time data interface, adopting a three-column layout: the left and right columns are dedicated to parameter configuration, while the middle column displays relevant data in real time under the current settings. Specifically, the left column is dedicated to inspection route planning and, in combination with the middle data panel, helps guide the robot to perform temperature measurements in designated "three-steel temperature" areas. The right-side settings interface allows for adjustments to key parameters such as travel speed, detection interval, and temperature alarm threshold.

4. Testing and Analysis

4.1 Laboratory Platform

A digital model of the cell was constructed using computer-aid 3D software, based on the cradle frame structure dimensions of a 400 kA cell from a certain smelter. As shown in Figure 5, the cradle frame model of the cell was built in the laboratory according to the specified structural dimensions. The robot inspection system was installed at the bottom of the H-beam to develop the inspection robot management program.



Figure 5. Simulation test platform for inspection robot operation.

By standardizing the measurement positions of the steel window, collector bar, and potshell bottom, and installing wireless infrared temperature probes for fixed-point temperature collection, the data are transmitted in real time to the central control system for analysis and storage. Through an integrated motion control strategy, the inspection robot achieves precise positioning and autonomous cruising along a preset path, simultaneously collecting, recording, and transmitting the three-steel temperature data in real time.

In the early stage of the experiment, the automatic calibration of the track's start and end points was achieved using the robot's self-check function. Based on the position signals provided by the inspection robot, the coordinates and dwell times of each measurement point were dynamically allocated.

Table 1. Comparison of infrared temperature measurement and patch-type temperature measurement.

Serial number	Patch-type thermocouple (°C)	Infrared temperature probe (°C)	Absolute error (°C)	Relative error
1	89.8	90.1	0.3	0.33 %
2	130.6	130	0.6	0.46 %
3	180.5	181.4	0.9	0.50 %
4	220.7	221.3	0.6	0.27 %
5	260.8	261.2	0.4	0.15 %
6	300.2	301.1	0.9	0.30 %

A 20 mm-thick steel plate was used to simulate the cell sidewall, with a resistance heating device installed to simulate the heat source. At the same monitoring point on the steel plate, real-time synchronous measurements were taken using the inspection robot's online infrared temperature

sensor and a patch-type thermocouple. As shown in Table 1, the simulation test results indicate that the online infrared temperature sensor of the inspection robot has a measurement accuracy of ± 1 °C.

4.2 Industrial Test

A robot inspection system was installed on the H-beam load-bearing beam at the bottom of the B-side of electrolytic cell 0122 at a certain plant (Figure 6). Ten groups of steel window structures between the two cradle frames were standardized and named (B1–B10). The aluminium alloy track was fixed to the lower flange of the H-beam using a suspended installation process. The track's working surface integrates a precision transmission device to ensure the stable operation of the inspection robot along the preset task path (Figure 6, right).



Figure 6. Synchronized measurement by manual and inspection robots.

The inspection robot can identify the start and end markers above the track, enabling equipment self-check and reset functions. In the early stage of the test, the robot's movement positions were recorded based on the centre marks of the measurement areas, and the inspection route was planned and set through the host computer interface.

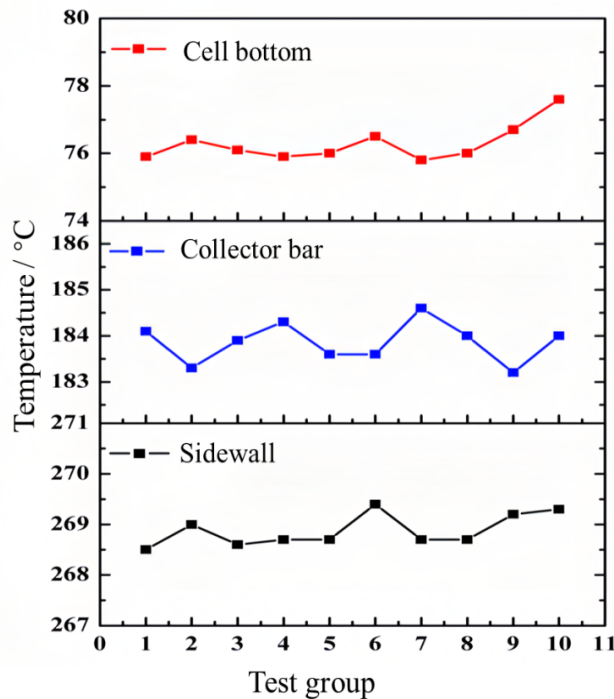


Figure 7. Test data of inspection robot at the same point.

As shown in Figure 7, the B4 position of the test cell was selected, and ten groups of repeatability tests were conducted by the inspection system to measure the temperature of the steel window, collector bar, and potshell bottom. The steel window temperature data showed a maximum of 269.4 °C, a minimum of 268.5 °C, an average of 268.88 °C, and a range of 0.9 °C. For the collector bar, the maximum temperature was 184.6 °C, the minimum was 183.2 °C, the average was 183.86 °C, and the range was 1.4 °C; The potshell bottom temperature ranged from 76.7 to 77.7 °C, with an average of 76.97 °C and a range of 1 °C.

As shown in Figures 8–10, the temperature of the steel window, collector bar, and potshell bottom was measured using a handheld infrared thermometer. After three repeated measurements, it was found that due to deviations in point location, distance, and angle in manual measurements, the data dispersion for the steel window, collector bar, and potshell bottom temperatures was significantly higher. In comparison, the inspection robot's temperature measurements for the steel window, collector bar, and potshell bottom showed an 88.7 % reduction in average data dispersion.

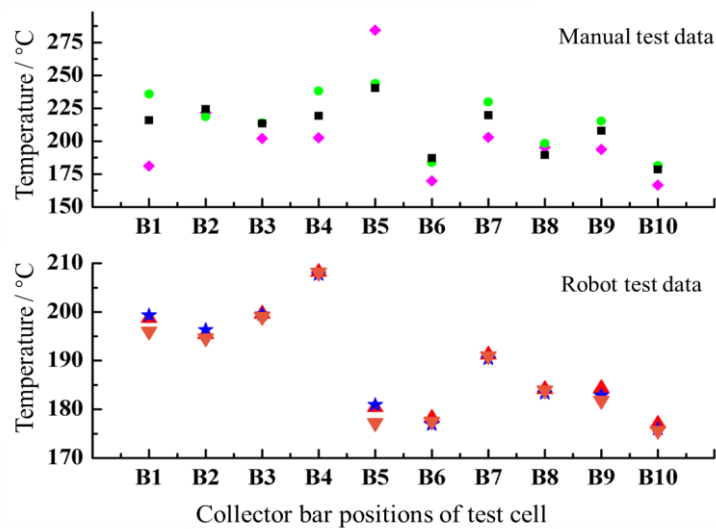


Figure 8. Comparison of inspection robot and manual test data at different collector bar points.

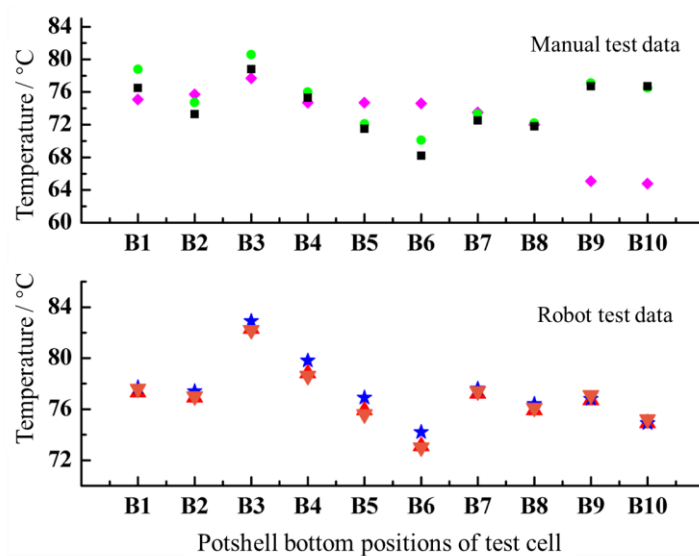


Figure 9. Comparison of inspection robot and manual test data at different potshell bottom points.

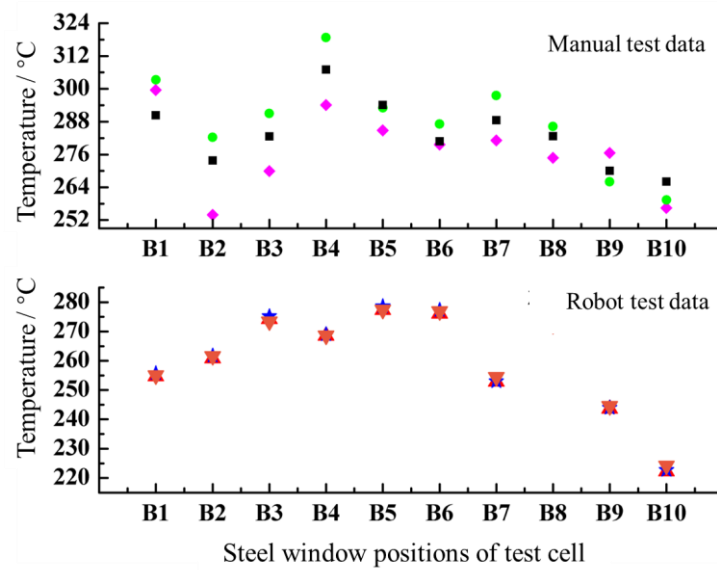


Figure 10 Comparison of inspection robot and manual test data at different steel window points.

A comparative analysis of the repeated temperature measurement data by manual and inspection robot methods (Tables 2, 3) revealed the following: For manual measurements, the maximum temperature ranges for the collector bar, steel window, and potshell bottom were 54.6 °C, 28.4 °C, and 12 °C respectively, with standard deviations of 10.24, 6.34, and 2. The corresponding maximum ranges measured by the inspection robot were 4.3 °C, 2.2 °C, and 3.9 °C, with standard deviations of 0.86, 0.55, and 0.71 respectively. Compared to manual measurements, the robot significantly reduced the maximum temperature ranges, and the average standard deviation decreased from 6.2 to 0.7, indicating improved measurement accuracy and greater reliability of the results.

Table 2. Comparison of maximum temperature range between manual and robot tests.

Measurement site	Maximum range of manual measurement (°C)	Maximum range of robot measurement (°C)	variation range
Collector bar	54.6	4.3	-92%
Steel window	28.4	2.2	-92%
Potshell bottom	12.0	3.9	-68%

Table 3. Comparison of standard deviation of temperature data between manual and robot tests.

Measurement site	Standard deviation of manual measurement(°C)	Standard deviation of robot measurement(°C)	variation range
Collector bar	10.24	0.86	-92%
Steel window	6.34	0.55	-91%
Potshell bottom	2.00	0.71	-65%

Based on the timing calculations during the inspection process, the inspection robot takes an average of 5 seconds to perform a three-steel temperature inspection at a single steel window in a 400 kA electrolytic cell. Consequently, the total inspection time required to cover all 48 steel

windows and 144 marked points along the side of the cell is only 240 seconds. Manual completion of temperature measurements at the same points requires two people working in coordination to test and record data, taking approximately 960 seconds. Therefore, the inspection system improves efficiency by 300 % compared to traditional manual inspection.

5. Conclusion and Outlook

The overhead rail inspection robot device and system proposed in this paper address the challenge of measuring the three-steel temperatures in aluminium electrolysis production, overcoming the bottlenecks of low efficiency, poor accuracy, and high environmental risks associated with traditional manual inspection. The device features an innovative suspended rail design, enabling autonomous cruising along a preset path in the narrow space at the bottom of the electrolytic cell. It integrates high-precision infrared temperature measurement and multi-sensor fusion technology to achieve fast and accurate detection of the three-steel temperature. Field test data from a 400 kA electrolytic cell at a certain enterprise show that the inspection system can cover all 48 steel windows and 144 inspection points in just 240 seconds, a 300 % improvement in efficiency compared to manual inspection. It achieves a positioning accuracy of ± 1 cm and a temperature measurement accuracy of ± 1 °C. Compared to manual measurement, the average standard deviation of the data decreased from 6.2 to 0.7, reducing data dispersion by 88.7 %.

Test results indicate that the overhead rail inspection technology for the cells offers significant advantages over traditional manual and ground-based inspection methods in terms of temperature measurement efficiency, accuracy, and safety. This technology helps improve the intelligence level of aluminium electrolysis production, reduces labour costs and safety risks, and provides technical support for multi-dimensional early warning diagnostics and the optimization of process control for the three-steel temperatures in the cells.

6. References

1. Zhuxian Qiu, *Principles and Applications of Aluminium Electrolysis*, Xuzhou, 1998, 8–26 (in Chinese).
2. Zhenjun Tan et al., Modelling of Cell Shell Temperature Monitoring and Analysis System for Aluminium Reduction Cells, *Light Metals*, Vol. 1, (2023), 23–27 (in Chinese).
3. Yu Hou et al., Research on the Application of Infrared Thermal Imaging Temperature Monitoring Technology in Aluminium Reduction Cells, *Metallurgical Automation*, Issue 39, Vol. 1, (2015), 67–71 (in Chinese).
4. Lei Wang et al., Inspection Robot Technology for Aluminium Electrolysis Cells, *Intelligent Mining*, Issue 3, Vol. 12, (2015), 58–61 (in Chinese).
5. Haibo Xia, Early Detection Application of Fiber Optic Temperature Measurement System for Aluminium Reduction Cell Leakage, *Communication Power Technology*, Issue 40, Vol. 9, (2023), 10–13 (in Chinese).
6. Yanbiao Liao, *Fiber Optics: Principles and Applications*, Beijing: Tsinghua University Press, (2010), 131–139 (in Chinese).
7. Yunlei Li et al., Development and Application of Online Three-Steel Temperature Measurement System for Aluminium Reduction Cells, *Yunnan Metallurgy*, Issue 53, Vol. 4, (2024), 171–175 (in Chinese).
8. Bottom Inspection Robot Developed by CITIC Heavy Industries Successfully Applied in Electrolytic Aluminium Industry, *Energy Saving in Nonferrous Metallurgy*, Issue 36, Vol. 3, (2020), 70–71 (in Chinese).
9. Zheng Liu et al., Research and Application of Online Cell Shell Temperature Detection System for Aluminium Reduction Cells, *Light Metals*, Vol. 1, (2007), 28–30 (in Chinese).